

Investigation of Flight Technical Error for UAV Separation Requirement Based on Flight Trajectory Data

Bizhao Pang^{*}, Mingcheng Zhang[†], Chao Deng[‡] and Kin Huat Low[§]

With the fast development of unmanned aircraft vehicle (UAV) operations in urban environments, the low-altitude air traffic is projected to be crowded. That would bring about problems such as how to determine the safe separation between two UAV operations. This paper proposes an evaluation framework for the determination of flight technical error (FTE) by investigating flight trajectory deviations, which is to support the establishment of separation requirement for UAV operations. Flight experiments are conducted by using a commonly used drone to collect flight trajectory data. Statistical analysis methods are used to investigate the trajectory deviations on lateral, longitudinal, and vertical axes. The normality tests are first conducted for the trajectory deviation data. The analysis of variance (ANOVA) is then performed to test the homogeneity of sample variances, while the regression analysis is conducted to investigate potential trends of the trajectory deviations with the change of flight heights. Statistical testing results show that the mean trajectory deviation in different flight times has no significant difference, whereas the mean trajectory deviation increases with the increase of flight height. The results also show that the linear increasing trend is more evident for deviations on the lateral track, while the quadratic increasing trend of trajectory deviation dominates on the longitudinal track. The deviations on vertical track is not significant compared with the ones on lateral and longitudinal tracks. This study investigates the flight technical error by analyzing the flight trajectory deviations, which will support the determination of separation requirement for safe UAV operations in low-altitude urban airspace.

I. Introduction

UNMANNED Aircraft System (UAS) has been developing fast with a number of applications [1–3] such as parcel delivery [4, 5], traffic monitoring [6], and inspection in urban environments [7, 8]. The contradiction between huge demands of UAS operations and limited airspace supply becomes a big problem for UAS traffic management system [9–11]. To deal with this problem, a discrete and scalable traffic management framework (Fig. 1) for urban airspace management has been proposed [12–14]. With that framework, waypoint-based route network planning can be conducted to reduce airborne collision risk and to improve the utilization of urban airspace [15–20].

However, problem arises when it comes to conducting the route network planning, because the air block size in the network is difficult to determine [21–23]. Too large an air block is a waste of airspace resources [24], while too small will have safety risk issues, as drones in adjacent air blocks may collide with each other [25, 26]. The separation requirement between UAV operations becomes an essential challenge needed to be solved to strike a balance between the safety and efficiency of urban low-altitude air traffic [27–29]. This paper therefore will investigate the separation requirement for UAV operations using statistical methods based on flight trajectory deviation data. Specifically, this work will investigate two main problems: (1) Are the means and variances of UAV trajectory deviation statistically the same in different flight times at a certain significance level? (2) With the increase in flight height, is there any significant trend in the mean trajectory deviation?

Here, we define UAV trajectory deviation as the spatial deviation between actual trajectory and pre-planned trajectory [23]. We investigate three axes of UAV operations, namely lateral, longitudinal, and vertical axes. That is corresponding to the size of length (l), width (w) and height (h) of the airspace cube. To achieve this, one way is to obtain the standard deviation of specific drone operations, which can be obtained by analyzing historical flight data [30]. For instance, if we would like to achieve that drone is flying within the airspace cube at 99% of the time, the minimum obstacle

^{*}Ph.D. Candidate, School of Mechanical and Aerospace Engineering, Nanyang Technological University, 639798, Singapore.

[†]Ph.D. Candidate, School of Mechanical and Aerospace Engineering, Nanyang Technological University, 639798, Singapore.

[‡]Project Officer, Air Traffic Management Research Institute, Nanyang Technological University, 637460, Singapore.

[§]Professor, School of Mechanical and Aerospace Engineering, Nanyang Technological University, 639798, Singapore. Corresponding author: mkhlow@ntu.edu.sg



Fig. 1 Concept of AirMatrix for airspace management

clearance can be computed by $2 * 3\sigma = 6\sigma$ (Fig. 2). In this case, the obstacle clearance is equivalent to the separation requirement. To get the trusted standard deviation, we study if the means and variances of trajectory deviation are the same in different operations at different flight times. We conducted multiple flight experiments and collected flight trajectory data for analysis.

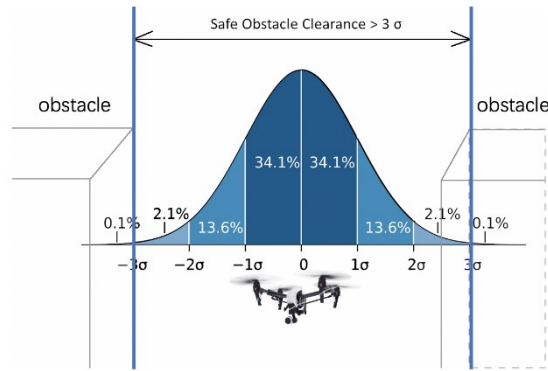


Fig. 2 Statistical correlation between separation requirement and flight trajectory deviation [31]

II. Methodology

The workflow of this paper is presented in Fig. 3. Data input includes five data sets of UAV flight trajectories with more than 50 data points. Each data point is taken as an average trajectory deviation in three seconds. We conduct the normality test for the obtained trajectory deviation data to see if the data is normally distributed. After that, we perform hypothesis testing and regression analysis to investigate the trajectory deviations in different experiment dates with different flight heights.

The normality-tested data will be used in two branches. First, we use the data to conduct hypothesis testing with null hypothesis H_0 and alternative hypothesis H_1 . The null hypothesis is presented as the population means from five testing days' data are statistically the same. While the alternative hypothesis is that not all the population means are the same. If H_0 is accepted, it means that there has statistically significant evidence that all flight experiments have the same standard deviation. If H_0 is rejected, we will perform post-hoc test to see which group of data has different σ causing the rejection. After identifying the abnormal observation, we can remove these outliers and continue to test the remaining samples. After iterations are completed, we can get the trusted standard deviation for separation requirement estimation.

The other branch is regression analysis. We first compute the predicated parameters for both linear trend and quadratic trend, and we then conduct tests to see if the two trends are significant. Next, we will compute the measure of association strength to see which trend is more dominant.

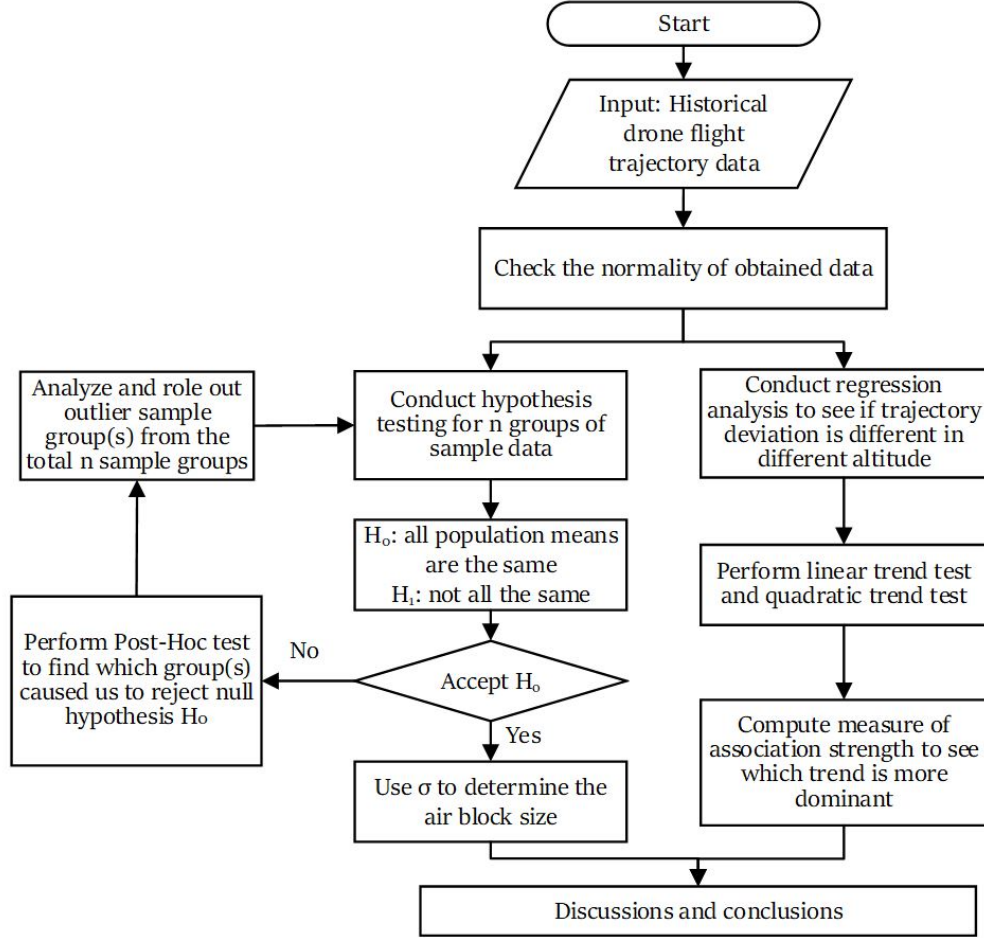


Fig. 3 Methodology of this work

A. Hypothesis Testing for Trajectory Sample Means

For the hypothesis testing, there are two independent variables: flight testing time and flight height. The dependent variable is the UAV flight trajectory deviation. They are presented as follows.

Independent variables are: (a) Testing date: Day 1, Day 2, Day 3, Day 4, and Day 5. (b) Flight height: 10 meters, 15 meters, and 20 meters. Dependent variable: Mean flight trajectory deviation.

We define μ_{i-j} as the sample mean for i th day of j th flight height. For instance, μ_{1-10} stands for the mean trajectory deviation of Day 1 at a flight height of 10 meters. Similarly, σ_{i-j}^2 is the variance of trajectory deviation for i th day of j th flight height. So, the hypothesis testing for the effect of different flight dates on trajectory deviation can be presented as:

- 1) Hypothesis (i) for population means.
 - $H_0: \mu_{1-10} = \mu_{2-10} = \mu_{3-10} = \mu_{4-10} = \mu_{5-10}$
 - $H_1: \text{Not all sample means are the same}$
- 2) Hypothesis (ii) for population variances.
 - $H_0: \sigma_{1-10}^2 = \sigma_{2-10}^2 = \sigma_{3-10}^2 = \sigma_{4-10}^2 = \sigma_{5-10}^2$
 - $H_1: \text{Not all sample variances are the same.}$

B. Regression Analysis on The Trend of Trajectory Deviation

The second part of this study is to conduct the regression analysis to see if there is a significant trend of trajectory deviation with the increase in flight height. The independent variables are flight heights, which are 10 meters, 15 meters, and 20 meters. The dependent variable is the flight trajectory deviation.

Independent variables are flight heights (x): 10 meters, 15 meters, and 20 meters. Dependent variable (y): Mean

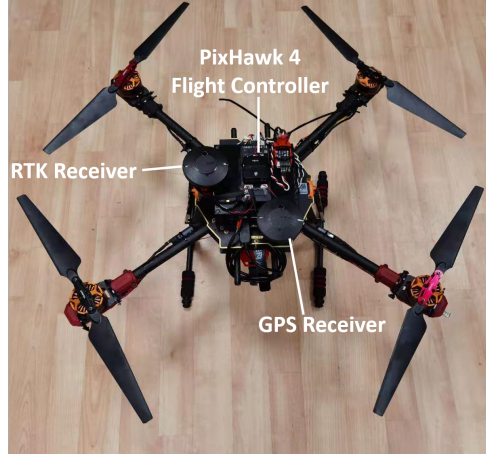


Fig. 4 The self-built drone used for flight experiments

flight trajectory deviation.

We conduct the linear trend analysis and quadratic trend analysis. The hypothesis test will also be performed to see if the trends are significant. The models for linear trend and quadratic trend are presented below.

- 1) Linear trend model: $y = \beta_0 + \beta_1 x$, $H_0 : \beta_1 = 0$, $H_1 : \beta_1 \neq 0$
- 2) Quadratic trend model: $y = \beta_0 + \beta_1 x + \beta_2 x^2$

After the computation of predicted parameters and hypothesis testing, the measure of association strength for each trend will also be computed to see which trend is more prominent.

III. Flight Experiments and Data Analysis with Normality and Homogeneity Tests

A. Settings for Flight Experiments and Data Collection

Five groups of sample data are obtained through experiment flights in the NTU campus on five different days. A self-built drone is used for flight experiments and data collection, which is illustrated as Fig. 4. The experiments are performed at three flight heights (10 meters, 15 meters, and 20 meters) and the same experiment procedure is conducted in five different days. The obtained flight trajectories are processed based on the reference trajectory, which is a pre-planned path that the UAV is supposed to follow. After processing, we obtain the UAV flight trajectory deviation data for each testing day at different flight heights.

B. Normality Test for Trajectory Deviations

- (1) Trajectory deviations on lateral axis

There are five days of testing data, and each day has three flight heights. We compute the mean and variance of these data and obtained results are given in Table 1. With the obtained data, we conduct the normality test using the *Lillietest* function. The MATLAB software is used in this analysis to perform the tests. The obtained histogram and Quantile-Quantile plot for normal distribution is given as Fig. 5. We also compute the statistical values and the obtained p-value is 0.4737, which is significantly greater than 0.05. We can conclude that the selected sample data is normally distributed at 0.05 significance level.

We conduct the same analysis for all trajectory deviation data at different flight heights and on three different axes. As the trajectory deviations on different axes are significantly different due to the flight dynamics, we perform the normality test for obtained data with three groups: lateral axis, longitudinal axis, and vertical axis. The obtained results are shown in Table 2 and Fig. 6.

As we can see from the results, all data has a p-value > 0.05, except for the trajectory deviation data on Day 4 at 15-meter flight height on lateral axis. The p-value of it is 0.0237 < 0.05. This part of data does not follow normal distribution at the 0.05 significance level. As we can also observed in Fig. 6, the red cycled sub-figure is more deviated from the normal reference line. This part of the data is cleaned out and will not involve in the following analysis.

- (2) Trajectory deviations on longitudinal axis

Table 1 Sample mean and variance of flight trajectory deviations

Test day	Flight height	Lateral axis		Longitudinal axis		Vertical axis	
		Mean (m)	Var. (m)	Mean (m)	Var. (m)	Mean (m)	Var. (m)
Day 1	10 m	5.0306	0.0379	3.6234	0.0647	0.1248	0.0058
	15 m	5.1346	0.0575	3.6554	0.0736	0.1623	0.0139
	20 m	5.4006	0.1089	3.7314	0.0804	0.1892	0.0151
Day 2	10 m	5.0386	0.0408	3.6260	0.0638	0.2015	0.0076
	15 m	5.1526	0.0569	3.6720	0.0699	0.1663	0.0065
	20 m	5.4086	0.0744	3.7280	0.0779	0.2193	0.0082
Day 3	10 m	5.0406	0.0439	3.6060	0.0794	0.0959	0.0040
	15 m	5.1306	0.0562	3.6580	0.0890	0.0988	0.0028
	20 m	5.4186	0.0944	3.7220	0.0830	0.1104	0.0020
Day 4	10 m	5.0546	0.0555	3.6434	0.0787	0.1698	0.0059
	15 m	5.1366	0.0689	3.6914	0.0951	0.2254	0.0048
	20 m	5.3666	0.1193	3.7514	0.1379	0.4228	0.0357
Day 5	10 m	5.0366	0.0695	3.6060	0.0696	0.1974	0.0166
	15 m	5.1786	0.0715	3.6040	0.0877	0.0734	0.0014
	20 m	5.3866	0.1586	3.6920	0.0896	0.4267	0.1136

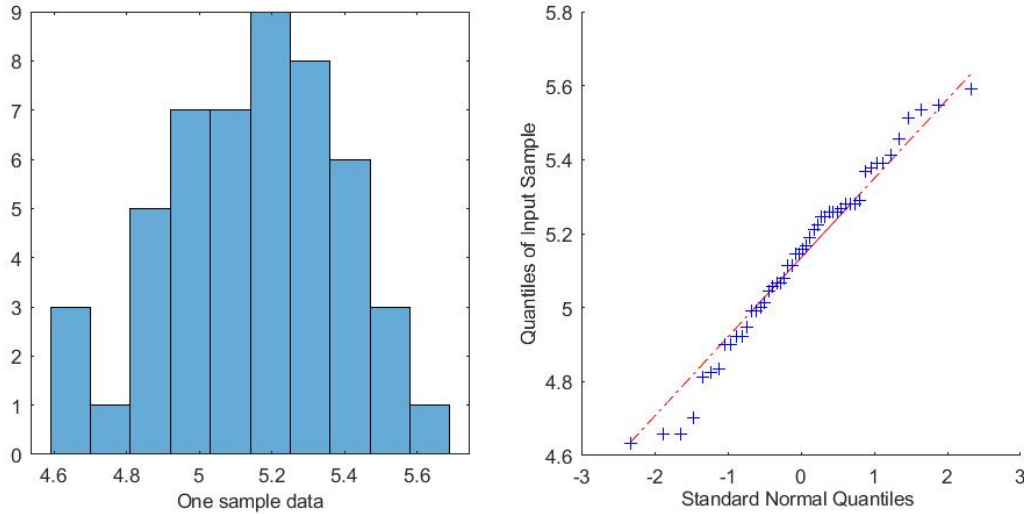


Fig. 5 An example of histogram and Quantile-Quantile plot for normal distribution

Table 2 P-values of normality test for three experiment group data ($p > 0.05 = \text{normal}$)

Axis	Lateral			Longitudinal			Vertical		
	10	15	20	10	15	20	10	15	20
Days/height (m)	10	15	20	10	15	20	10	15	20
Day 1	0.4737	0.5000	0.5000	0.3470	0.5000	0.0226	0.0448	0.0023	0.0010
Day 2	0.3936	0.5000	0.5000	0.5000	0.5000	0.1262	0.0323	0.2693	0.1317
Day 3	0.3807	0.2908	0.1641	0.1298	0.2987	0.3016	0.0149	0.1391	0.1216
Day 4	0.4767	0.0237	0.1611	0.5000	0.1246	0.5000	0.2907	0.0010	0.1938
Day 5	0.3246	0.5000	0.2977	0.5000	0.5000	0.3988	0.0082	0.0126	0.0038

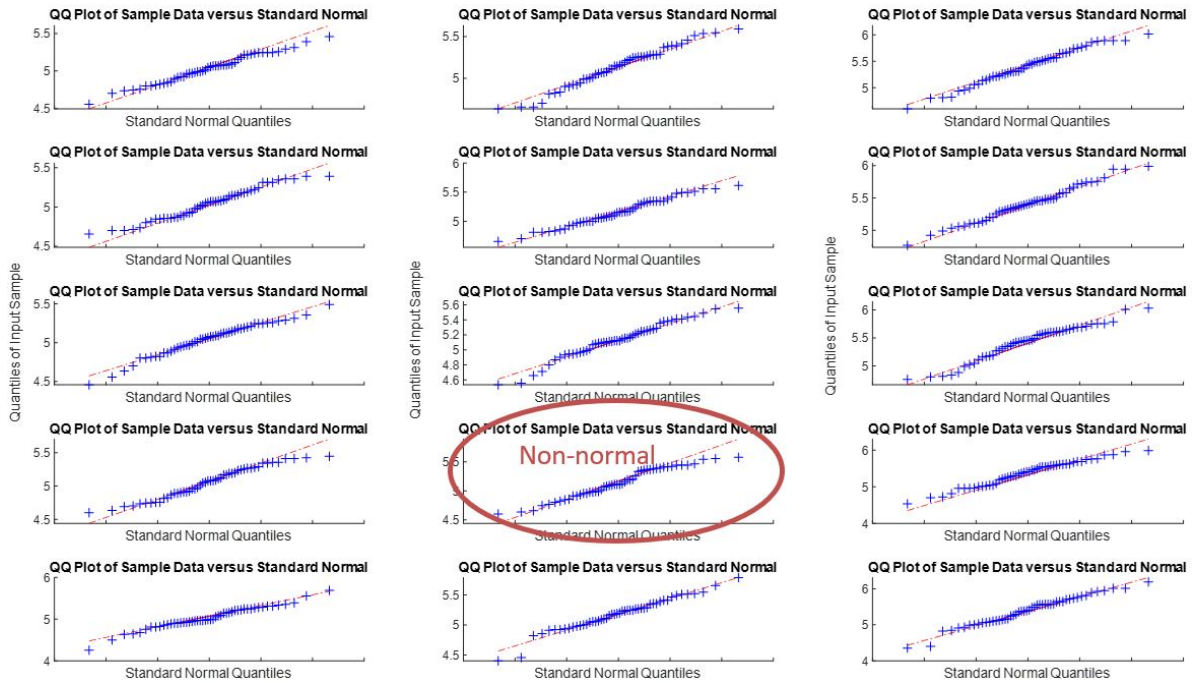


Fig. 6 Quantile-Quantile (Q-Q) Plot for normal distribution on lateral axis

In this part we test the normality for longitudinal group data and the obtained results are given in Table 2 and Fig. 7. As we can see, the only data set which has no significant normality is on Day 1 at 20 meters. The p-value for that data set is $0.0226 < 0.05$. We, therefore, remove that data set in the following analysis.

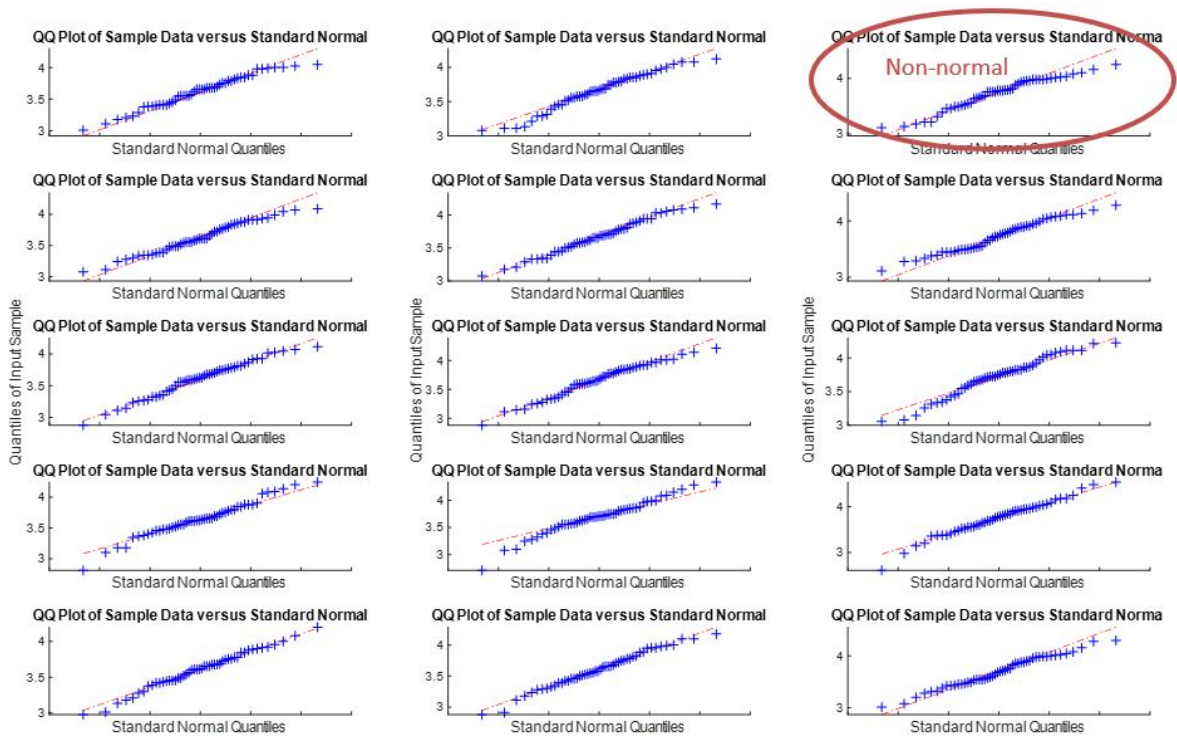


Fig. 7 Quantile-Quantile (Q-Q) Plot for normal distribution on longitudinal axis

(3) Trajectory deviations on vertical axis

We also test the normality for vertical group data. Quite differently, the vertical group data shows significantly less normality (see Fig. 8). This is because of UAV flight dynamics. On vertical axis, its performance is more stable and reliable than on lateral and longitudinal axes, thus having fewer deviations on vertical axis. The mean vertical deviation is around 0.2 meters, which is significantly smaller than the deviations on the other two axes (see Table 1). In the following hypothesis testing and regression analysis, we will therefore not involve the vertical group data.

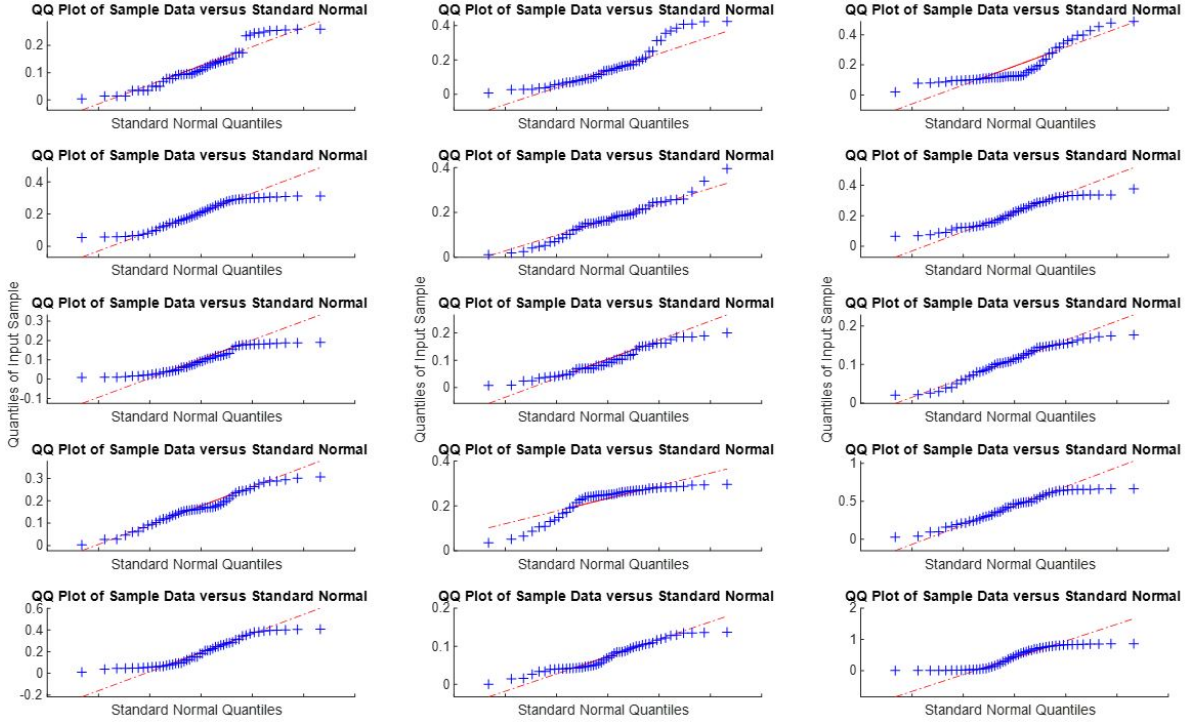


Fig. 8 Q-Q Plot for normal distribution on vertical axis

C. Homogeneity Test for Variance of Trajectory Deviation

The normality of all three groups' data has been tested in the above sections. In this section, we check if the obtained sample trajectory deviation data has an equal variance. The equal variance across samples is defined as homogeneity of variance, which is important in ANOVA testing. The violation of homogeneity of variance will have a great probability of falsely rejecting the null hypothesis, resulting in a false conclusion in ANOVA testing. To conduct the homogeneity test, the *Vartestn* function is used and the obtained test results are given in Fig. 9.

After the computation, we obtained that $p\text{-value}=0.1729 > 0.05$. We can conclude that the variance of the obtained trajectory deviation data in different days has no significant difference at 5% significance level.

IV. Hypothesis Testing and Regression Analysis

To investigate if the mean value of trajectory deviation in various flights has a significant difference at the same flight height, hypothesis testing is conducted. After that, the trend analysis is also performed to see if the mean value of deviation follows any trend with the increase in flight height.

A. Hypothesis Testing of Trajectory Deviation Means

In this part, we conduct one-way ANOVA to test if the trajectory deviations have a significant difference between five different testing days.

- 1) Hypothesis (i): for population means at a flight height of 10 meters

$$H_0: \mu_{1-10} = \mu_{2-10} = \mu_{3-10} = \mu_{4-10} = \mu_{5-10}$$

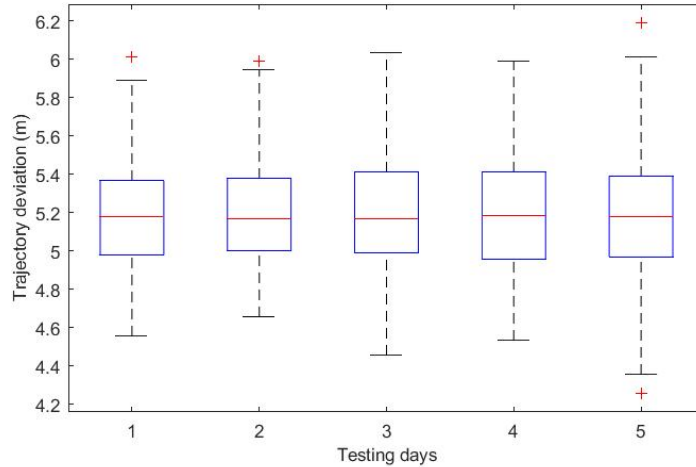


Fig. 9 Results of homogeneity test for variance

- H_1 : Not all the means are the same
- 2) Hypothesis (ii): for population means at a flight height of 15 meters
 $H_0: \mu_{1_15} = \mu_{2_15} = \mu_{3_15} = \mu_{4_15} = \mu_{5_15}$
 H_1 : Not all the means are the same
- 3) Hypothesis (iii): for population means at a flight height of 20 meters
 $H_0: \mu_{1_20} = \mu_{2_20} = \mu_{3_20} = \mu_{4_20} = \mu_{5_20}$
 H_1 : Not all the means are the same

After computation, the p-values at different flight heights are $p_{-10}=0.9885$, $p_{-15}=0.8688$, and $p_{-20}=0.9461$. As all p-values are greater than 0.05, we accept the null hypotheses that the population means at the same flight height on different testing days have no significant difference at the 0.05 significance level. The homogeneity test is also performed for the three groups of data, and there is no significant difference in variances between different samples. The results are presented in Fig. 10.

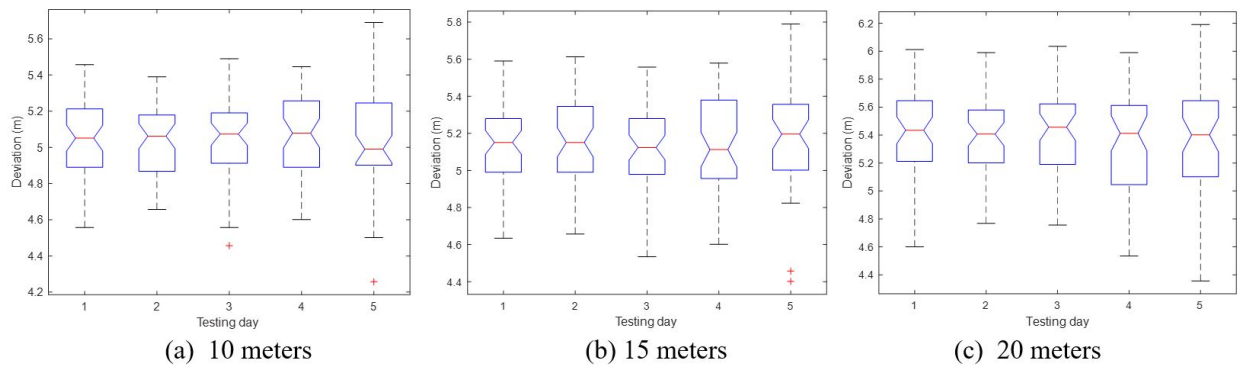


Fig. 10 Results of homogeneity test for sample variance

We also conducted the power of the test for these three hypotheses, and the observed power for lateral deviations is 0.66, while for longitudinal and vertical deviations are 0.53 and 0.58. As we can see the powers are relatively not satisfactory, and we can increase the power by adding more sample points.

B. Regression Analysis for Flight Deviations at Different Heights

In this part, we conduct the regression analysis to see if the means of trajectory deviation have any significant trend with the increase in flight height. As discussed above, we only analyze the data on lateral axis and longitudinal axis, because the deviations on the vertical axis is insignificant (less than 0.2 meters on average). In regression analysis, the

Table 3 Independent and observed dependent variables for regression analysis

Variables/Axis	Lateral			Longitudinal		
	x (m)	10	15	20	10	15
y (m)	5.0402	5.1466	5.3962	3.621	3.65615	3.725

independent variables are flight heights (x), which are 10, 15, and 20 meters. While the dependent variable (y) is the mean of trajectory deviation. The independent and observed dependent variables used in the regression analysis are given in Table 3.

First, we conduct a linear trend analysis and hypothesis test. The model is presented as:

$$y = \beta_0 + \beta_1 x$$

$$H_0 : \beta_1 = 0$$

$$H_1 : \beta_1 \neq 0$$

1. Regression Analysis for Lateral Trajectory Deviation

Based on the regression model, we compute the trend parameters of lateral trajectory deviation. We have $\beta_0 = 4.6603, \beta_1 = 0.0356$. Thus, the linear trend for lateral deviation can be denoted as $y = 4.6603 + 0.0356x$.

To test if the linear trend is significant, we perform the hypothesis test with null hypothesis is $H_0 : \beta_1 = 0$, while alternative hypothesis is $H_1 : \beta_1 \neq 0$. The obtained results are: $R^2 = 0.9488; F_{\text{obs}} = 18.5411 > F_{\text{crit}}((0.05, 1, 150 - 3 = 147)) = 3.84$. Based on the results, the observed F-value (18.5411) is greater than the significance F-value (3.84). We can conclude that the linear trend is significant at 0.05 significance level. We further conduct the quadratic analysis, and the obtained predicted formula is $y = 5.2570 - 0.0503x + 0.0029x^2$.

Finally, we compute the measure of association strength for both the linear and quadratic trends to see which trend is more prominent. Based on the computed measure of association strength, the quadratic trend is more dominant, with the strength of R^2_{alerting} being 55.69%.

We plot the predicted means based on a model that includes both linear and quadratic trend components, presented in Fig. 11. In general, the estimated means have a significant linear trend as we can see from the figure. The blue line is the estimated linear trend. The predicted means corresponding to the first and third heights are significantly close to the actual sample means. While for the second height, the predicted mean is greater than the actual sample mean. For the quadratic trend, we can see that the means are significantly close to the actual means for all three points. The deviation from quadratic means and actual sample means are not significant.

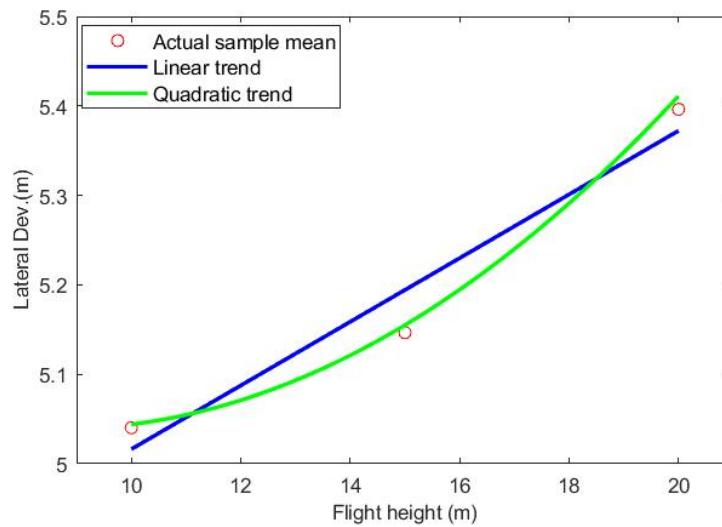


Fig. 11 Predicted means for both linear and quadratic trends on lateral axis

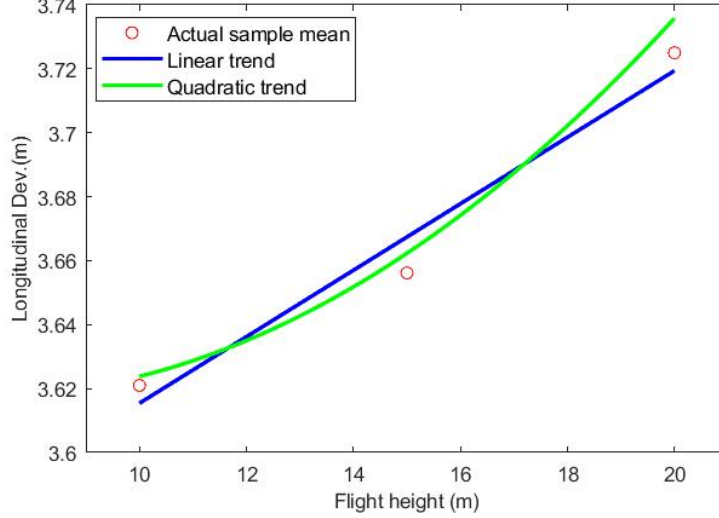


Fig. 12 Predicted means for both linear and quadratic trends on longitudinal axis

2. Regression Analysis for Longitudinal Trajectory Deviation

We conduct the same regression analysis for longitudinal trajectory deviation. We obtained the predicted parameters as $\beta_0 = 3.5114$, and $\beta_1 = 0.0104$. Thus, we have the predicted linear trend model $y = 3.5114 + 0.0104x$. The other obtained results are: $R^2 = 0.9662$; $F_{\text{obs}} = 28.5712 > F_{\text{crit}}((0.05, 1, 150 - 3 = 147)) = 3.84$. Based on the results, we can see that the observed F-value (28.5712) is greater than the significance F-value (3.84). We can conclude that the linear trend is significant at 0.05 significance level. We further conduct the quadratic analysis, and the obtained predicted formula is $y = 3.6518 - 0.0098x + 0.0007x^2$.

We compute the measure of association strength for both linear and quadratic trends. Based on the computed measure of association strength, we can see that the linear trend is more dominant, though not strong, for the sample data with R^2_{alerting} is 53.03%. This is also more evident than the linear trend for these data with 46.97% of R^2_{alerting} .

We plot the predicted means based on a model that includes both linear and quadratic trend components, presented in Fig. 12. In general, the estimated means have a significant linear trend. The blue line is the estimated linear trend. The predicted means correspond to the first and third heights are significantly close to the actual sample means. While for the second height, the predicted mean is greater than the actual sample mean. For the quadratic trend, the first point of mean is significantly close to the actual mean, while the other two do not close to the actual means.

C. Result Discussion on the Determination of Separation Requirement

After the above tests and analysis, we can see that the obtained trajectory data follow the normal distribution at a 0.05 significance level, while the obtained data on different testing days at different flight heights have the same means and variances. It can be concluded that the flight trajectory deviation is consistent in different flight times and flight heights for a specific UAV. The obtained flight deviation can be used to determine the separation requirement. Based on the analysis in Fig. 2, we know the size of the air block on one particular axis is six times of its standard deviation (6σ) on that axis at 0.01 significance level. Therefore, we can compute the separation requirement on each axis, and the results are shown in Table 4. The separation requirement means that a UAV operating in such size of air block will have 99% of the time does not fly out of the air block. Note that the obtained size of the air block in this study is only applicable for the particular drone used in the experiment flights, and it does not consider any safety buffer and protection zone. A practical and implementable separation requirement would require the consideration of a certain safety buffer, while the analysis for more flight trajectory data of various types of drones will help specific UAV operations and risk assessment.

V. Conclusions

This paper studies the UAV separation requirement using statistical methods with real-world flight experiment data. Hypothesis tests are conducted to test the means and variances of sample trajectory deviation data. The regression

Table 4 Estimated separation requirement for a specific drone at 0.01 significance level

Parameters	Lateral	Longitudinal
Variance (m)	5.19	3.67
Standard deviation (m)	2.28	1.92
Separation requirement (m)	14	11

analysis is also performed to investigate the trend of the trajectory deviation with the increase of the flight height. The main findings of this paper can be concluded as follows.

- 1) The trajectory deviation of UAV flight at the same height follows normal distribution when the sample size is 50 at a 0.05 significance level. The trajectory deviations in different testing days at different flights height also follow the normal distribution, which has the same variance.
- 2) The means of trajectory deviations on different testing days are statistically the same at a 0.05 significance level. This indicates the time of a flight has no significant impact on the mean trajectory deviations for a particular drone.
- 3) With the increase in flight height, the trajectory deviations on lateral and longitudinal axes will increase. The linear increasing trend is more evident in lateral deviation while the quadratic trend dominates in longitudinal deviation.

The research findings of this paper rely on the obtained flight experiment data in a specific environment with a particular drone. In future works, more experiments can be conducted with other types of UAV and flight environments to collect more sample data that can be used for UAV separation requirement analysis. Moreover, separation requirements for flights with payloads (e.g., parcel delivery case) can also be investigated, as the payloads may serve as a damper to mitigate the deviation effect or act as a booster to amplify the deviation due to inertia effects.

VI. Acknowledgment

This research is supported by the National Research Foundation, Singapore, and the Civil Aviation Authority of Singapore, under the Aviation Transformation Programme. Any opinions, findings and conclusions or recommendations expressed in this material are those of the authors and do not reflect the views of National Research Foundation, Singapore and the Civil Aviation Authority of Singapore. The Research Student Scholarship provided by the Nanyang Technological University to the first and second authors is acknowledged. The authors would also like to thank Mr. Ee Meng Ng for his support in part of the flight experiments.

References

- [1] FAA, and NASA, "FAA UTM Concept of Operations - v1.0," Tech. rep., 2018. URL <https://utm.arc.nasa.gov/docs/2018-UTM-ConOps-v1.0.pdf>.
- [2] FAA, and NASA, "FAA UTM Concept of Operations - v2.0," Tech. rep., 2020. URL https://www.faa.gov/uas/research_development/traffic_management/media/UTM_ConOps_v2.pdf.
- [3] Pang, B., Wang, C. H. J., and Low, K. H., "Framework of Level-of-Autonomy-based Concept of Operations : UAS Capabilities," *2021 IEEE/AIAA 40th Digital Avionics Systems Conference (DASC)*, 2021. URL <https://hdl.handle.net/10356/151831>.
- [4] Huang, H., Savkin, A. V., and Huang, C., "Reliable Path Planning for Drone Delivery Using a Stochastic Time-Dependent Public Transportation Network," *IEEE Transactions on Intelligent Transportation Systems*, 2020, pp. 1–10. <https://doi.org/10.1109/TITS.2020.2983491>.
- [5] Blom, H. A., Jiang, C., Grimme, W. B., Mitici, M., and Cheung, Y. S., "Third party risk modelling of Unmanned Aircraft System operations, with application to parcel delivery service," *Reliability Engineering and System Safety*, Vol. 214, 2021, p. 107788. <https://doi.org/10.1016/j.res.2021.107788>.
- [6] Lin, C. E., Hsieh, C.-S., Li, C.-C., Shao, P.-C., Lin, Y.-H., and Yeh, Y.-C., "An ADS-B like communication for UTM," *Integrated Communications, Navigation and Surveillance Conference, ICNS*, Vol. 2019-April, IEEE, 2019, pp. 1–12. <https://doi.org/10.1109/ICNSURV.2019.8735199>.

- [7] Hu, X., Pang, B., Dai, F., and Low, K. H., "Risk Assessment Model for UAV Cost-Effective Path Planning in Urban Environments," *IEEE Access*, Vol. 8, 2020, pp. 150162–150173. <https://doi.org/10.1109/ACCESS.2020.3016118>.
- [8] Pang, B., Hu, X., Dai, W., and Low, K. H., "UAV Path Optimization with An Integrated Cost Assessment Model Considering Third-Party Risks in Metropolitan Environments," *Reliability Engineering and System Safety*, 2022, pp. 1–18. <https://doi.org/https://doi.org/10.1016/j.res.2022.108399>.
- [9] Battista, A., and Ni, D., "A Comparison of Traffic Organization Methods for Small Unmanned Aircraft Systems," *Transportation Research Record*, Vol. 2672, No. 23, 2018, pp. 20–30. <https://doi.org/10.1177/0361198118757995>.
- [10] Jiang, T., Geller, J., Ni, D., and Collura, J., "Unmanned Aircraft System traffic management: Concept of operation and system architecture," *International Journal of Transportation Science and Technology*, Vol. 5, No. 3, 2016, pp. 123–135. <https://doi.org/10.1016/j.ijst.2017.01.004>.
- [11] Doole, M., Ellerbroek, J., and Hoekstra, J., "Estimation of traffic density from drone-based delivery in very low level urban airspace," *Journal of Air Transport Management*, Vol. 88, 2020, p. 101862. <https://doi.org/10.1016/j.jairtraman.2020.101862>.
- [12] Tan, Q., Wang, Z., Ong, Y. S., and Low, K. H., "Evolutionary optimization-based mission planning for UAS traffic management (UTM)," *2019 International Conference on Unmanned Aircraft Systems, ICUAS 2019*, 2019, pp. 952–958. <https://doi.org/10.1109/ICUAS.2019.8798078>.
- [13] Pang, B., Dai, W., Ra, T., and Low, K. H., "A Concept of Airspace Configuration and Operational Rules for UAS in Current Airspace," *2020 IEEE/AIAA 39th Digital Avionics Systems Conference (DASC)*, IEEE, 2020, pp. 1–9. <https://doi.org/10.1109/DASC50938.2020.9256627>.
- [14] Wu, Y., Low, K. H., Pang, B., and Tan, Q., "Swarm-based 4D Path Planning for Drone Operations in Urban Environments," *IEEE Transactions on Vehicular Technology*, Vol. 9545, No. c, 2021. <https://doi.org/10.1109/TVT.2021.3093318>.
- [15] Ding, W., Gao, W., Wang, K., and Shen, S., "An Efficient B-Spline-Based Kinodynamic Replanning Framework for Quadrotors," *IEEE Transactions on Robotics*, Vol. 35, No. 6, 2019, pp. 1287–1306. <https://doi.org/10.1109/TRO.2019.2926390>.
- [16] Wang, C. H., Tan, S. K., and Low, K. H., "Three-dimensional (3D) Monte-Carlo modeling for UAS collision risk management in restricted airport airspace," *Aerospace Science and Technology*, Vol. 105, 2020, p. 105964. <https://doi.org/10.1016/j.ast.2020.105964>.
- [17] Pang, B., Tan, Q., Ra, T., and Low, K. H., "A Risk-based UAS Traffic Network Model for Adaptive Urban Airspace Management," *AIAA Aviation Forum*, AIAA, 2020, pp. 1–9. <https://doi.org/10.2514/6.2020-2900>.
- [18] Pang, B., Dai, W., Hu, X., Dai, F., and Low, K. H., "Multiple air route crossing waypoints optimization via artificial potential field method," *Chinese Journal of Aeronautics*, Vol. 34, No. 4, 2021. <https://doi.org/10.1016/j.cja.2020.10.008>.
- [19] Dai, W., Pang, B., and Low, K. H., "Conflict-free four-dimensional path planning for urban air mobility considering airspace occupancy," *Aerospace Science and Technology*, Vol. 119, 2021, p. 107154. <https://doi.org/10.1016/j.ast.2021.107154>.
- [20] Zou, Y., Zhang, H., Zhong, G., Liu, H., and Feng, D., "Collision probability estimation for small unmanned aircraft systems," *Reliability Engineering and System Safety*, Vol. 213, 2021, p. 107619. <https://doi.org/10.1016/j.res.2021.107619>.
- [21] Bojia, Y., and Shortle, J. F., "Collision risk-capacity tradeoff analysis of an en-route corridor model," *Chinese Journal of Aeronautics*, Vol. 27, No. 1, 2014, pp. 124–135. <https://doi.org/10.1016/j.cja.2013.12.007>.
- [22] Daniel, B. J., and Verma, A., "Likelihood of Unmitigated Collision Risks for Uas in Defined Airspace Volumes," *Integrated Communications, Navigation and Surveillance Conference, ICNS*, Vol. 2020-Septe, 2020, pp. 1–7. <https://doi.org/10.1109/ICNS50378.2020.9222872>.
- [23] Wang, C. H. J., Ng, E. M., and Low, K. H., "Investigation and Modeling of Flight Technical Error (FTE) Associated with UAS Operating with and without Pilot Guidance," *IEEE Transactions on Vehicular Technology*, 2021, pp. 1–13. <https://doi.org/10.1109/TVT.2021.3117081>.
- [24] Xue, M., "Three-Dimensional Sector Design with Optimal Number of Sectors," *Journal of Guidance, Control, and Dynamics*, Vol. 35, 2012, pp. 609–618. <https://doi.org/10.2514/1.51979>.
- [25] Hoekstra, J. M., Maas, J., Tra, M., and E., S., "How Do Layered Airspace Design Parameters Affect Airspace Capacity and Safety?" 2016. URL https://pure.tudelft.nl/ws/portalfiles/portal/87262684/ICRAT_2016_paper_6.pdf.

- [26] Brittain, M. W., Yang, X., and Wei, P., “Autonomous Separation Assurance with Deep Multi-Agent Reinforcement Learning,” *Journal of Aerospace Information Systems*, 2021, pp. 1–16. <https://doi.org/10.2514/1.i010973>.
- [27] Wu, Y., Li, L. L., Su, X., and Gao, B., “Dynamics modeling and trajectory optimization for unmanned aerial-aquatic vehicle diving into the water,” *Aerospace Science and Technology*, Vol. 89, 2019, pp. 220–229. <https://doi.org/10.1016/j.ast.2019.04.004>.
- [28] Pang, B., Low, K. H., and Lv, C., “Adaptive conflict resolution for multi-UAV 4D routes optimization using stochastic fractal search algorithm,” *Transportation Research Part C: Emerging technology*, 2022. <https://doi.org/10.1016/j.trc.2022.103666>.
- [29] Wu, P., Yang, X., Wei, P., and Chen, J., “Safety Assured Online Guidance With Airborne Separation for Urban Air Mobility Operations in Uncertain Environments,” *IEEE Transactions on Intelligent Transportation Systems*, 2022, pp. 1–15. <https://doi.org/10.1109/TITS.2022.3163657>.
- [30] Khan, M. A., Ectors, W., Bellemans, T., Janssens, D., and Wets, G., “UAV-Based Traffic Analysis: A Universal Guiding Framework Based on Literature Survey,” *Transportation Research Procedia*, Vol. 22, No. 2016, 2017, pp. 541–550. <https://doi.org/10.1016/j.trpro.2017.03.043>.
- [31] Deng, C., Wang, C. H. J., and Low, K. H., “Investigation of Using Sky Openness Ratio as Predictor for Navigation Performance in Urban-like Environment to Support PBN in UTM,” *Sensors*, Vol. 22, 2022. <https://doi.org/10.3390/s22030840>.